

Articles

Synthesis, Structural Characterization, and Catalytic Property of Group 4 Metal Carborane Compounds with a ${}^i\text{Pr}_2\text{NB}$ -Bridged Constrained-Geometry Ligand

Guofu Zi, Hung-Wing Li, and Zuowei Xie*

Department of Chemistry, The Chinese University of Hong Kong, Shatin,
New Territories, Hong Kong, China

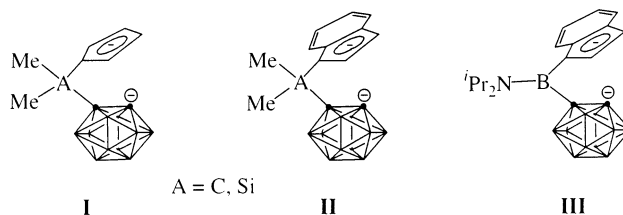
Received April 23, 2002

Interaction of ${}^i\text{Pr}_2\text{NB}(\text{C}_9\text{H}_7)(\text{C}_2\text{B}_{10}\text{H}_{11})$ with 1 equiv of $\text{Zr}(\text{NMe}_2)_4$ gave a constrained-geometry zirconium amide $[\eta^5\text{-}\sigma\text{-}{}^i\text{Pr}_2\text{NB}(\text{C}_9\text{H}_6)(\text{C}_2\text{B}_{10}\text{H}_{10})]\text{Zr}(\text{NMe}_2)_2$ (**2**). Treatment of ${}^i\text{Pr}_2\text{NB}(\text{C}_9\text{H}_7)(\text{C}_2\text{B}_{10}\text{H}_{11})$ with 1 equiv of $\text{Ti}(\text{NMe}_2)_4$, however, led to the isolation of a deborated product $(\eta^5\text{-}\text{C}_2\text{B}_9\text{H}_{11})\text{Ti}(\text{NMe}_2)_2(\text{HNMe}_2)$ (**1**). **2** reacted with excess Me_3SiCl in toluene to give the chloro derivative $[\eta^5\text{-}\sigma\text{-}{}^i\text{Pr}_2\text{NB}(\text{C}_9\text{H}_6)(\text{C}_2\text{B}_{10}\text{H}_{10})]\text{ZrCl}_2$ (**4**). Salt metathesis reaction between $\text{MCl}_4(\text{THF})_2$ and $[\eta^5\text{-}\sigma\text{-}{}^i\text{Pr}_2\text{NB}(\text{C}_9\text{H}_6)(\text{C}_2\text{B}_{10}\text{H}_{10})]\text{Li}_2(\text{Et}_2\text{O})_2$ afforded $[\eta^5\text{-}\sigma\text{-}{}^i\text{Pr}_2\text{NB}(\text{C}_9\text{H}_6)(\text{C}_2\text{B}_{10}\text{H}_{10})]\text{MCl}_2$ ($\text{M} = \text{Ti}$ (**3**), Zr (**4**), Hf (**5**)). **3** was also prepared from the reaction of $[\eta^5\text{-}\sigma\text{-}{}^i\text{Pr}_2\text{NB}(\text{C}_9\text{H}_6)(\text{C}_2\text{B}_{10}\text{H}_{10})]\text{Li}_2(\text{Et}_2\text{O})_2$ with 1 equiv of $\text{TiCl}_3(\text{THF})_3$, followed by addition of 0.5 equiv of PbCl_2 in THF. Interaction of **2** with 4 equiv of Me_3Al in toluene resulted in the isolation of $[\eta^5\text{-}\sigma\text{-}{}^i\text{Pr}_2\text{NB}(\text{C}_9\text{H}_6)(\text{C}_2\text{B}_{10}\text{H}_{10})]\text{ZrMe}_2$ (**6**). **6** was also prepared via the reaction of **4** with 2 equiv of MeLi in THF. All of these compounds were fully characterized by various spectroscopic data and elemental analyses. The solid-state structures of compounds **1** and **2** were further confirmed by single-crystal X-ray analyses. Compounds **2–6** exhibited a moderate to very high ($10^4\text{--}10^6 \text{ g mol}^{-1} \text{ atm}^{-1} \text{ h}^{-1}$) ethylene polymerization activity upon activation with MAO. The activities depended upon both the central metal ion and co-ligand and followed the order **4** > **2**, **6** > **3** > **5**.

Introduction

Ligand modifications have played a key role in developing new catalyst precursors for optimizing polymerization activity as well as polymer properties such as stereoregularity, molecular weight, bulky and polar comonomer incorporation, and microstructure.¹ Boron-bridged *ansa*-ligands have recently attracted much attention since the electrophilic boron-linkage may affect the property of the active metal center via geometry changes and intramolecular Lewis acid coactivation.² Two classes of compounds have been studied: (1) metallocenes bridged by three-coordinate boron moieties where the electrophilicity of boron is attenuated by a partial $\text{p}_\pi\text{-p}_\pi$ π -bonding³ and (2) metallocenes bridged with four-coordinate boron-linkages.⁴ Experimental results show that the R_2NB -bridged *ansa*-

Chart 1. Constrained-Geometry Carboranyl Ligands



ligands can offer metallocenes with a very high activity in polymerization/copolymerization of α -olefins.^{3,c,d} We have recently developed a ${}^i\text{Pr}_2\text{NB}$ -bridged carboranyl constrained-geometry ligand bearing a carboanion functionality (Chart 1, III).⁵ Our recent results show that zirconocenes derived from ligands I and II (Chart 1) exhibit a very high activity in ethylene polymerization.⁶ Given the impact of boron-bridged constrained-geometry ligands³ and carboranyl moieties^{6,7} on the catalytic performance of the group 4 metal compounds, we have extended our research to a newly developed ${}^i\text{Pr}_2\text{NB}$ -bridged system in the hope that the electrophilic boron-linkage together with the electron-deficient carborane moiety can enhance the Lewis acidity of the central metal ions, which then in turn increases the catalytic activity of the catalysts. We report herein our detailed

* Corresponding author. Fax: (852)26035057. Tel: (852)26096269. E-mail: zxie@cuhk.edu.hk.

(1) For reviews, see: (a) Britovsek, G. J. P.; Gibson, V. C.; Wass, D. F. *Angew. Chem., Int. Ed.* **1999**, *38*, 428. (b) Kaminsky, W.; Arndt, M. *Adv. Polym. Sci.* **1997**, *127*, 144. (c) Bochmann, M. *J. Chem. Soc., Dalton Trans.* **1996**, 255. (d) Kaminsky, W. *Macromol. Chem. Phys.* **1996**, *197*, 3907. (e) Brintzinger, H. H.; Fisher, D.; Mülhaupt, R.; Rieger, B.; Waymouth, R. M. *Angew. Chem., Int. Ed. Engl.* **1995**, *34*, 1143. (f) Möhring, R. C.; Coville, N. J. *J. Organomet. Chem.* **1994**, *479*, 1. (g) Marks, T. J. *Acc. Chem. Res.* **1992**, *25*, 57. (h) Jordan, R. F. *Adv. Organomet. Chem.* **1991**, *32*, 325.

(2) For a recent review, see: Shapiro, P. J. *Eur. J. Inorg. Chem.* **2001**, 321.

study on this subject. The similarities and differences among group 4 metal compounds with B-, C-, and Si-bridged ligands are also discussed in this paper.

Experimental Section

General Procedures. All experiments were performed under an atmosphere of dry dinitrogen with the rigid exclusion of air and moisture using standard Schlenk or cannula techniques, or in a glovebox. All organic solvents (except CH₂-Cl₂) were freshly distilled from sodium benzophenone ketyl immediately prior to use. CH₂Cl₂ was freshly distilled from CaH₂ immediately prior to use. M(NMe₂)₄ (M = Ti, Zr),⁸ ¹Pr₂-NB(C₉H₇)(C₂B₁₀H₁₁),⁵ and [¹Pr₂NB(C₉H₆)(C₂B₁₀H₁₀)]Li₂(OEt₂)₂⁵ were prepared according to literature methods. All other chemicals were purchased from either Aldrich or Acros Chemical Co. and used as received unless otherwise noted. Infrared spectra were obtained from KBr pellets prepared in the glovebox on a Perkin-Elmer 1600 Fourier transform spectrometer. Molecular weights of the polymer were estimated by gel permeation chromatography (GPC) using a PL-GPC 200 high-temperature GPC (Polymer Laboratories Ltd.). ¹H and ¹³C NMR spectra were recorded on a Bruker DPX 300 spectrometer at 300.13 and 75.47 MHz, respectively. ¹¹B NMR spectra were recorded on a Varian Inova 400 spectrometer at 128.32 MHz. All chemical shifts were reported in δ units with references to the residual protons of the deuterated solvents for proton and carbon chemical shifts and to external BF₃·OEt₂ (0.00 ppm) for boron chemical shifts. Elemental analyses were performed by MEDAC Ltd., Brunel University, Middlesex, U.K.

Preparation of (η⁵-C₂B₉H₁₁)Ti(NMe₂)₂(HNMe₂) (1). A toluene solution (10 mL) of ¹Pr₂NB(C₉H₇)(C₂B₁₀H₁₁) (0.37 g,

1.00 mmol) was slowly added to a toluene solution (10 mL) of Ti(NMe₂)₄ (0.22 g, 1.00 mmol) with stirring at room temperature. The reaction mixture was heated to 65 °C and stirred overnight to give a deep red solution. The solution was filtered and concentrated to about 5 mL, from which **1** was isolated as brick-red crystals after this solution stood at room temperature for several days (0.09 g, 29%). ¹H NMR (pyridine-*d*₅): δ 3.47 (s, 12H, NCH₃), 3.25 (br s, 2H, cage CH), 2.34 (s, 6H, HNCH₃), proton of HNMe₂ was not observed. ¹³C NMR (pyridine-*d*₅): δ 56.43 (C₂B₉H₁₁), 51.01 (NCH₃), 40.53 (HNCH₃). ¹¹B NMR (pyridine-*d*₅): δ 6.1 (1B), -4.9 (2B), -5.6 (2B), -15.1 (3B), -20.7 (1B). IR (KBr, cm⁻¹): ν 3223 (m), 2955 (m), 2901 (s), 2858 (m), 2535 (vs), 1455 (s), 1258 (s), 1095 (vs), 1023 (vs), 803 (s). Anal. Calcd for C₈H₃₀B₉N₃Ti: C, 30.65; H, 9.65; N, 13.41. Found: C, 30.13; H, 9.69; N, 13.01.

Preparation of [η⁵-σ-¹Pr₂NB(C₉H₆)(C₂B₁₀H₁₀)]Zr(NMe₂)₂ (2). A toluene solution (10 mL) of ¹Pr₂NB(C₉H₇)(C₂B₁₀H₁₁) (0.37 g, 1.00 mmol) was slowly added to a toluene solution (10 mL) of Zr(NMe₂)₄ (0.27 g, 1.00 mmol) with stirring at room temperature. The reaction mixture was heated to 65 °C and stirred overnight to give a yellow solution. This solution was filtered and concentrated to about 3 mL, from which **2** was isolated as yellow crystals after this solution stood at room temperature for several days (0.38 g, 70%). ¹H NMR (pyridine-*d*₅): δ 7.69 (d, *J* = 8.4 Hz, 1H, indenyl), 7.23 (t, *J* = 7.2 Hz, 1H, indenyl), 7.10 (t, *J* = 7.2 Hz, 1H, indenyl), 6.65 (d, *J* = 8.4 Hz, 1H, indenyl), 6.64 (d, *J* = 2.4 Hz, 1H, indenyl), 6.03 (d, *J* = 2.4 Hz, 1H, indenyl), 5.32 (m, 1H, NCHMe₂), 3.28 (m, 1H, NCHMe₂), 2.99 (s, 6H, NCH₃), 2.32 (s, 6H, NCH₃), 1.22 (d, *J* = 6.3 Hz, 3H, NCH(CH₃)₂), 1.20 (d, *J* = 6.3 Hz, 3H, NCH(CH₃)₂), 0.98 (d, *J* = 6.3 Hz, 3H, NCH(CH₃)₂), 0.55 (d, *J* = 6.3 Hz, 3H, NCH(CH₃)₂). ¹³C NMR (pyridine-*d*₅): δ 130.8, 128.0, 126.8, 126.2, 126.0, 125.6, 125.3, 104.8, 103.6 (indenyl), 88.6 (cage C), 51.0, 49.4 (NCHMe₂), 47.4, 45.9 (NCH₃), 27.1, 26.5, 24.0, 23.1 (NCH(CH₃)₂). ¹¹B NMR (pyridine-*d*₅): δ 0.3 (1B), -1.8 (1B), -5.1 (3B), -9.0 (4B), -10.9 (2B). IR (KBr, cm⁻¹): ν 2959 (m), 2909 (vs), 2576 (vs), 1491 (s), 1259 (s), 1096 (vs), 1026 (vs), 801 (s). Anal. Calcd for C₂₁H₄₂B₁₁N₃Zr: C, 46.13; H, 7.74; N, 7.69. Found: C, 46.21; H, 7.83; N, 7.50.

Preparation of [η⁵-σ-¹Pr₂NB(C₉H₆)(C₂B₁₀H₁₀)]TiCl₂ (3). To a THF (10 mL) solution of TiCl₄(THF)₂ (0.33 g, 1.00 mmol) was slowly added a THF (10 mL) solution of [¹Pr₂NB(C₉H₆)(C₂B₁₀H₁₀)]Li₂(OEt₂)₂ (0.53 g, 1.00 mmol) with stirring at -78 °C. The reaction mixture was warmed to room temperature and stirred overnight. The solvent was evaporated under vacuum. The oily residue was extracted with CH₂Cl₂ (10 mL × 3). The CH₂Cl₂ solutions were combined and concentrated to about 5 mL, to which *n*-hexane (15 mL) was added. **3** was isolated as red microcrystals after this solution stood at room temperature for several days (0.19 g, 40%). ¹H NMR (pyridine-*d*₅): δ 8.01 (d, *J* = 7.8 Hz, 1H, indenyl), 7.81 (d, *J* = 7.8 Hz, 1H, indenyl), 7.12 (d, *J* = 3.0 Hz, 1H, indenyl), 6.97 (t, *J* = 8.1 Hz, 1H, indenyl), 6.87 (t, *J* = 8.1 Hz, 1H, indenyl), 6.65 (d, *J* = 3.0 Hz, 1H, indenyl), 5.70 (m, 1H, NCHMe₂), 3.65 (m, 1H, NCHMe₂), 1.35 (d, *J* = 6.3 Hz, 3H, NCH(CH₃)₂), 1.32 (d, *J* = 6.3 Hz, 3H, NCH(CH₃)₂), 1.30 (d, *J* = 6.3 Hz, 3H, NCH(CH₃)₂), 1.17 (d, *J* = 6.3 Hz, 3H, NCH(CH₃)₂). ¹³C NMR (benzene-*d*₆): δ 130.4, 129.2, 124.7, 124.3, 121.1, 120.5, 114.5, 114.3, 94.7 (indenyl), 82.1 (cage C), 49.0, 48.4 (NCHMe₂), 26.4, 26.3, 23.5, 22.8 (NCH(CH₃)₂). ¹¹B NMR (pyridine-*d*₅): δ -1.5 (1B), -3.7 (1B), -6.8 (3B), -10.8 (4B), -11.3 (2B). IR (KBr, cm⁻¹): ν 3058 (w), 2960 (s), 2915 (s), 2547 (vs), 1454 (s), 1385 (s), 1260 (s), 1088 (vs), 1027 (vs), 802 (s). Anal. Calcd for C₁₇H₃₀B₁₁Cl₂NTi: C, 42.00; H, 6.22; N, 2.88. Found: C, 41.87; H, 6.13; N, 2.67.

Alternate Method. To a suspension of TiCl₃(THF)₃ (0.37 g, 1.00 mmol) in THF (15 mL) was slowly added a THF (10 mL) solution of [¹Pr₂NB(C₉H₆)(C₂B₁₀H₁₀)]Li₂(OEt₂)₂ (0.53 g, 1.00 mmol) with stirring at -78 °C. The reaction mixture was slowly allowed to warm to room temperature and stirred overnight. To the resulting green solution was added PbCl₂ (0.14 g, 0.50 mmol) as a powder at room temperature. An

(3) (a) Braunschweig, H.; Dirk, R.; Müller, M.; Nguyen, P.; Resendes, R.; Gates, D. P.; Manners, I. *Angew. Chem., Int. Ed. Engl.* **1997**, *36*, 2338. (b) Braunschweig, H.; von Koblinski, C.; Wang, R. *Eur. J. Inorg. Chem.* **1999**, 69. (c) Ashe, A. J.; Fang, X.; Kampf, J. W. *Organometallics* **1999**, *18*, 2288. (d) Braunschweig, H.; von Koblinski, C.; Englert, U. *J. Chem. Soc., Chem. Commun.* **2000**, 1049. (e) Duchateau, R.; Lancaster, S. J.; Thornton-Pett, M.; Bochmann, M. *Organometallics* **1997**, *16*, 4995. (f) Braunschweig, H.; von Koblinski, C.; Neugebauer, M.; Englert, U.; Zheng, X. *J. Organomet. Chem.* **2001**, *619*, 305. (g) Knizek, J.; Krossing, I.; Nöth, H.; Ponikvar, W. *Eur. J. Inorg. Chem.* **1998**, 505, 5. (h) Patton, J. T.; Feng, S. G. *Organometallics* **2001**, *20*, 3399. (i) Braunschweig, H.; von Koblinski, C.; Mamuti, M.; Englert, U.; Wang, R. *Eur. J. Inorg. Chem.* **1999**, 1899. (j) Rufanov, K. A.; Kotov, V. V.; Kazennova, N. B.; Lemenovskii, D. A.; Avtomonov, E. V.; Lorberth, J. *J. Organomet. Chem.* **1996**, *525*, 287. (k) Rufanov, K.; Avtomonov, E.; Kazennova, N.; Kotov, V.; Khvorost, A.; Lemenovskii, D.; Lorberth, J. *J. Organomet. Chem.* **1997**, *536-537*, 361. (l) Larkin, S. A.; Golden, J. T.; Shapiro, P. J.; Yap, G. P. A.; Foo, D. M. J.; Rheingold, A. L. *Organometallics* **1996**, *15*, 2393.

(4) (a) Stelck, D. S.; Shapiro, P. J.; Basickes, N.; Rheingold, A. L. *Organometallics* **1997**, *16*, 4546. (b) Reetz, M. T.; Willuhn, M.; Psiorz, C.; Goddard, R. *J. Chem. Soc., Chem. Commun.* **1999**, 1105. (c) Lancaster, S. J.; Al-Benna, S.; Thornton-Pett, M.; Bochmann, M. *Organometallics* **2000**, *19*, 1599. (d) Lancaster, S. J.; Thornton-Pett, M.; Dawson, D. M.; Bochmann, M. *Organometallics* **1998**, *17*, 3829. (e) Lancaster, S. J.; Bochmann, M. *Organometallics* **2001**, *20*, 2093. (f) Bochmann, M.; Lancaster, S. J.; Robinson, O. B. *J. Chem. Soc., Chem. Commun.* **1995**, 2081. (g) Burns, C. T.; Stelck, D. S.; Shapiro, P. J.; Vij, A.; Kunz, K.; Kehr, G.; Concolino, T.; Rheingold, A. L. *Organometallics* **1999**, *18*, 5432. (h) Burlakov, V. V.; Arndt, P.; Baumann, W.; Spannenberg, A.; Rosenthal, U.; Letov, A. V.; Lysenko, K. A.; Korlyukov, A. A.; Strunkina, L. I.; Minacheva, M. Kh.; Shur, V. B. *Organometallics* **2001**, *20*, 4072.

(5) Zi, G.; Li, H.-W.; Xie, Z. *Organometallics* **2002**, *21*, 1136.

(6) Wang, H.; Wang, Y.; Li, H.-W.; Xie, Z. *Organometallics* **2001**, *20*, 5110.

(7) (a) Dodge, T.; Curtis, M. A.; Russell, J. M.; Sabat, M.; Finn, M. G.; Grimes, R. N. *J. Am. Chem. Soc.* **2000**, *122*, 10573. (b) Kim, D.-H.; Won, J. H.; Kim, S.-J.; Ko, J.; Kim, S.-H.; Cho, S.; Kang, S. O. *Organometallics* **2001**, *20*, 4298. (c) Grassi, A.; Maffei, G.; Millione, S.; Jordan, R. F. *Macromol. Chem. Phys.* **2001**, *202*, 1239. (d) Crowther, D. J.; Baenziger, N. C.; Jordan, R. F. *J. Am. Chem. Soc.* **1991**, *113*, 1455. (e) Crowther, D. J.; Jordan, R. F. *Makromol. Chem., Macromol. Symp.* **1993**, *66*, 121.

(8) Diamond, G. M.; Jordan, R. F.; Petersen, J. L. *J. Am. Chem. Soc.* **1996**, *118*, 8024.

immediate color change to red with gradual precipitation of Pb⁰ was observed. The reaction mixture was stirred at room temperature for 4 h, followed by the procedures used above to give **3** as red microcrystals (0.17 g, 35%).

Preparation of [$\eta^5\text{-}\sigma\text{-Pr}_2\text{NB}(\text{C}_9\text{H}_6)(\text{C}_2\text{B}_{10}\text{H}_{10})\text{]ZrCl}_2$ (4**).**

A toluene solution (10 mL) of Me₃SiCl (0.54 g, 5.00 mmol) was slowly added to a toluene (20 mL) solution of **2** (0.55 g, 1.00 mmol) with stirring at -20 °C, and the mixture was slowly warmed to room temperature and stirred overnight. The solvent was evaporated under vacuum. The oily residue was extracted with CH₂Cl₂ (10 mL × 3). The CH₂Cl₂ solutions were combined and concentrated to about 8 mL, to which *n*-hexane (15 mL) was added. **4** was isolated as pale yellow microcrystals after this solution stood at room temperature for several days (0.42 g, 80%). ¹H NMR (pyridine-*d*₅): δ 8.04 (d, *J* = 7.2 Hz, 1H, indenyl), 7.80 (d, *J* = 7.2 Hz, 1H, indenyl), 7.15 (d, *J* = 3.0 Hz, 1H, indenyl), 7.00 (t, *J* = 6.3 Hz, 1H, indenyl), 6.87 (t, *J* = 6.3 Hz, 1H, indenyl), 6.68 (d, *J* = 3.0 Hz, 1H, indenyl), 5.72 (m, 1H, NCHMe₂), 3.44 (m, 1H, NCHMe₂), 1.35 (d, *J* = 6.3 Hz, 3H, NCH(CH₃)₂), 1.33 (d, *J* = 6.3 Hz, 3H, NCH(CH₃)₂), 1.31 (d, *J* = 6.3 Hz, 3H, NCH(CH₃)₂), 1.18 (d, *J* = 6.3 Hz, 3H, NCH(CH₃)₂). ¹³C NMR (pyridine-*d*₅): δ 129.7, 126.9, 125.7, 125.0, 124.9, 124.4, 124.2, 103.7, 102.5 (indenyl), 88.8 (cage C), 49.9, 48.3 (NCHMe₂), 26.0, 25.4, 22.9, 22.0 (NCH(CH₃)₂). ¹¹B NMR (pyridine-*d*₅): δ -2.5 (1B), -4.6 (1B), -8.0 (3B), -11.9 (4B), -14.1 (2B). IR (KBr, cm⁻¹): ν 2939 (s), 2564 (vs), 1473 (vs), 1368 (s), 1272 (w), 1031 (vs), 814 (s). Anal. Calcd for C₁₇H₃₀B₁₁Cl₂Nzr: C, 38.56; H, 5.71; N, 2.65; Cl, 13.39. Found: C, 38.56; H, 5.77; N, 2.88; Cl, 13.72.

Alternate Method. This compound was also prepared as pale yellow microcrystals from the reaction of ZrCl₄(THF)₂ (0.38 g, 1.00 mmol) with [²Pr₂NB(C₉H₆)(C₂B₁₀H₁₀)]Li₂(OEt)₂ (0.53 g, 1.00 mmol) in THF (20 mL) using procedures similar to those used in the synthesis of **3**: yield 0.24 g (46%).

Preparation of [$\eta^5\text{-}\sigma\text{-Pr}_2\text{NB}(\text{C}_9\text{H}_6)(\text{C}_2\text{B}_{10}\text{H}_{10})\text{]HfCl}_2$ (5**).**

This compound was prepared as colorless microcrystals from the reaction of HfCl₄(THF)₂ (0.46 g, 1.00 mmol) and [²Pr₂NB(C₉H₆)(C₂B₁₀H₁₀)]Li₂(OEt)₂ (0.53 g, 1.00 mmol) in THF (20 mL) using procedures similar to those used in the synthesis of **3**: yield 0.34 g (56%). ¹H NMR (pyridine-*d*₅): δ 7.98 (d, *J* = 8.1 Hz, 1H, indenyl), 7.71 (d, *J* = 8.1 Hz, 1H, indenyl), 7.12 (d, *J* = 3.0 Hz, 1H, indenyl), 6.90 (t, *J* = 6.6 Hz, 1H, indenyl), 6.81 (t, *J* = 6.6 Hz, 1H, indenyl), 6.61 (d, *J* = 3.0 Hz, 1H, indenyl), 5.66 (m, 1H, NCHMe₂), 3.45 (m, 1H, NCHMe₂), 1.26 (d, *J* = 6.3 Hz, 3H, NCH(CH₃)₂), 1.22 (d, *J* = 6.3 Hz, 3H, NCH(CH₃)₂), 1.18 (d, *J* = 6.3 Hz, 3H, NCH(CH₃)₂), 1.12 (d, *J* = 6.3 Hz, 3H, NCH(CH₃)₂). ¹³C NMR (pyridine-*d*₅): δ 130.3, 129.0, 128.7, 124.9, 121.2, 120.5, 114.6, 114.3, 94.7 (indenyl), 82.1 (cage C), 49.0, 48.4 (NCHMe₂), 26.4, 26.3, 23.5, 22.8 (NCH(CH₃)₂). ¹¹B NMR (pyridine-*d*₅): δ -1.7 (1B), -3.4 (1B), -6.9 (3B), -11.4 (6B). IR (KBr, cm⁻¹): ν 3062 (w), 2924 (s), 2868 (s), 2586 (vs), 1614 (m), 1453 (s), 1272 (m), 1075 (s), 886 (s), 802 (s), 733 (s). Anal. Calcd for C₁₇H₃₀B₁₁Cl₂HfN: C, 33.11; H, 4.90; N, 2.27. Found: C, 32.89; H, 4.85; N, 2.36.

Preparation of [$\eta^5\text{-}\sigma\text{-Pr}_2\text{NB}(\text{C}_9\text{H}_6)(\text{C}_2\text{B}_{10}\text{H}_{10})\text{]ZrMe}_2$ (6**).**

A 2.0 M solution of AlMe₃ in *n*-hexane (2.0 mL, 4.0 mmol) was slowly added to a toluene (20 mL) solution of **2** (0.55 g, 1.00 mmol) with stirring at -20 °C, resulting in the formation of a yellow precipitate. This suspension was then stirred at room temperature overnight. The precipitate was collected and washed with *n*-hexane (20 mL × 3), giving **6** as a yellow solid (0.38 g, 78%). ¹H NMR (pyridine-*d*₅): δ 7.87 (d, *J* = 6.0 Hz, 1H, indenyl), 7.34 (d, *J* = 6.0 Hz, 1H, indenyl), 7.18 (t, *J* = 9.0 Hz, 1H, indenyl), 6.98 (t, *J* = 9.0 Hz, 1H, indenyl), 6.36 (d, *J* = 6.0 Hz, 1H, indenyl), 6.14 (d, *J* = 6.0 Hz, 1H, indenyl), 5.37 (m, 1H, NCHMe₂), 3.32 (m, 1H, NCHMe₂), 1.25 (d, *J* = 6.0 Hz, 3H, NCH(CH₃)₂), 1.21 (d, *J* = 6.0 Hz, 3H, NCH(CH₃)₂), 1.16 (d, *J* = 6.0 Hz, 3H, NCH(CH₃)₂), 0.58 (d, *J* = 6.0 Hz, 3H, NCH(CH₃)₂), -0.38 (s, 6H, ZrCH₃). ¹³C NMR (pyridine-*d*₅): δ 131.4, 126.7, 126.4, 126.1, 122.6, 120.2, 106.0, 100.5, 98.2 (indenyl), 91.9 (cage C), 49.7, 48.7 (NCHMe₂), 43.0 (ZrCH₃),

Table 1. Crystal Data and Summary of Data Collection and Refinement for **1 and **2****

	1	2
formula	C ₈ H ₃₀ B ₉ N ₃ Ti	C ₂₁ H ₄₂ B ₁₁ N ₃ Zr
cryst size (mm)	0.46 × 0.39 × 0.31	0.65 × 0.60 × 0.56
fw	313.5	546.7
cryst syst	monoclinic	monoclinic
space group	<i>P</i> 2 ₁ / <i>n</i>	<i>P</i> 2 ₁
<i>a</i> , Å	8.847(1)	9.436(1)
<i>b</i> , Å	12.298(1)	15.829(1)
<i>c</i> , Å	16.931(2)	10.562(1)
β, deg	105.15	110.80(1)
<i>V</i> , Å ³	1778.2(3)	1474.8(2)
<i>Z</i>	4	2
<i>D</i> _{calcd} , Mg/m ³	1.171	1.231
radiation (λ), Å	Mo Kα (0.71073)	Mo Kα (0.71073)
2θ range, deg	4.1 to 56.2	4.6 to 56.1
μ, mm ⁻¹	0.470	0.389
<i>F</i> (000)	664	568
no. of obsd reflns	4318	5169
no. of params refnd	203	327
goodness of fit	1.038	1.041
R1	0.048	0.023
wR2	0.153	0.067

25.9, 25.3, 23.2, 23.0 (NCH(CH₃)₂). ¹¹B NMR (pyridine-*d*₅): δ -1.4 (1B), -3.2 (1B), -6.6 (3B), -11.0 (6B). IR (KBr, cm⁻¹): ν 3060 (w), 2961 (vs), 2904 (s), 2582 (vs), 1454 (s), 1381 (s), 1255 (s), 1089 (vs), 1029 (vs), 797 (s). Anal. Calcd for C₁₉H₃₆B₁₁NZr: C, 46.70; H, 7.43; N, 2.87. Found: C, 46.37; H, 7.53; N, 3.01.

Alternate Method. A 1.5 M solution of MeLi in Et₂O (1.4 mL, 2.1 mmol) was slowly added to a THF (15 mL) solution of **4** (0.53 g, 1.00 mmol) with stirring at -78 °C. The reaction mixture was warmed to room temperature and stirred overnight. This solution was filtered and concentrated to about 10 mL, to which *n*-hexane (10 mL) was added. **6** was isolated as yellow microcrystals after this solution stood at room temperature for several days (0.27 g, 56%).

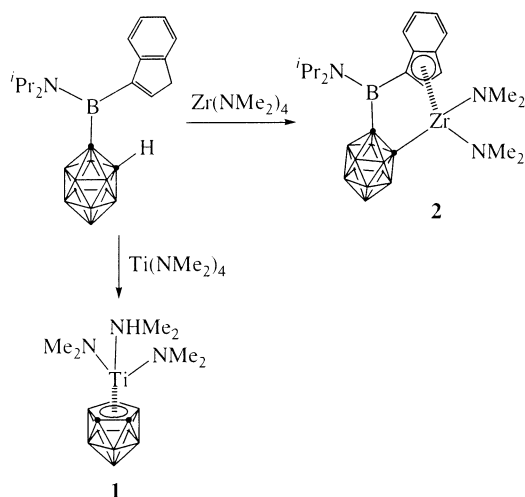
Ethylene Polymerization. This experiment was carried out in a 150 mL glass reactor equipped with a magnetic stirrer and gas inlets. The reactor was charged with the catalyst together with MAO and toluene (50 mL). The mixture was stirred at room temperature for 1 h. Ethylene gas was then introduced to the reactor, and its pressure was maintained continuously at 1 atm by means of bubbling. The polymerization was terminated by addition of acidic ethanol (100 mL). The white precipitate was filtered off and washed with ethanol and acetone. The resulting powder was finally dried in a vacuum oven at 80 °C overnight.

X-ray Structure Determination. All single crystals were immersed in Paraton-N oil and sealed under N₂ in thin-walled glass capillaries. Data were collected at 293 K on a Bruker SMART 1000 CCD diffractometer using Mo Kα radiation. An empirical absorption correction was applied using the SADABS program.⁹ All structures were solved by direct methods and subsequent Fourier difference techniques and refined anisotropically for all non-hydrogen atoms by full-matrix least-squares calculations on *F*² using the SHELXTL program package.^{10a} For the non-centrosymmetric structure **2**, the appropriate enantiomorph was chosen by refining Flack's parameter *x* toward zero.^{10b} Most of the carborane hydrogen atoms were located from difference Fourier syntheses. All other hydrogen atoms were geometrically fixed using the riding model. Crystal data and details of data collection and structure refinements are given in Table 1. Further details are included in the Supporting Information.

(9) Sheldrick, G. M. *SADABS*: Program for Empirical Absorption Correction of Area Detector Data; University of Göttingen: Germany, 1996.

(10) (a) Sheldrick, G. M. *SHELXTL 5.10 for Windows NT*: Structure Determination Software Programs; Bruker Analytical X-ray Systems, Inc.: Madison, WI, 1997. (b) Flack, H. D. *Acta Crystallogr.* **1983**, *A39*, 876.

Scheme 1

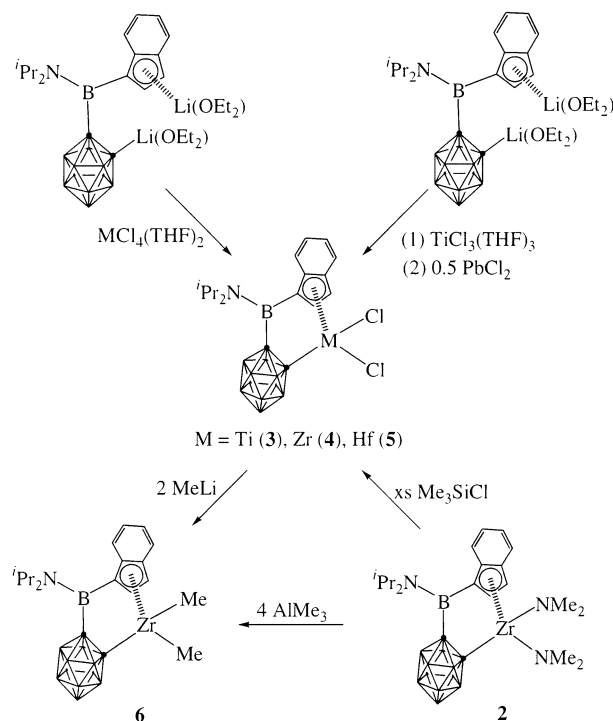


Results and Discussion

Synthesis. Our previous work showed that interaction between $\text{Me}_2\text{A}(\text{C}_9\text{H}_7)(\text{C}_2\text{B}_{10}\text{H}_{11})$ or $\text{Me}_2\text{A}(\text{C}_5\text{H}_5)(\text{C}_2\text{B}_{10}\text{H}_{11})$ ($\text{A} = \text{C}, \text{Si}$) and $\text{M}(\text{NMe}_2)_4$ in toluene resulted in the clean formation of the corresponding organo group 4 metal amide compounds.⁶ The two acidic protons in $\text{Pr}_2\text{NB}(\text{C}_9\text{H}_7)(\text{C}_2\text{B}_{10}\text{H}_{11})$ would allow similar amine elimination to occur between $\text{Pr}_2\text{NB}(\text{C}_9\text{H}_7)(\text{C}_2\text{B}_{10}\text{H}_{11})$ and metal amides. In fact, treatment of $\text{Pr}_2\text{NB}(\text{C}_9\text{H}_7)(\text{C}_2\text{B}_{10}\text{H}_{11})$ with 1 equiv of $\text{Zr}(\text{NMe}_2)_4$ in toluene at 65 °C gave the desired compound $[\eta^5\text{-}\sigma\text{-Pr}_2\text{NB}(\text{C}_9\text{H}_7)(\text{C}_2\text{B}_{10}\text{H}_{11})]\text{Zr}(\text{NMe}_2)_2$ (**2**) in 70% yield. Under similar reaction conditions, however, interaction between $\text{Pr}_2\text{NB}(\text{C}_9\text{H}_7)(\text{C}_2\text{B}_{10}\text{H}_{11})$ and an equimolar amount of $\text{Ti}(\text{NMe}_2)_4$ in toluene did not lead to the isolation of the expected compound $[\eta^5\text{-}\sigma\text{-Pr}_2\text{NB}(\text{C}_9\text{H}_7)(\text{C}_2\text{B}_{10}\text{H}_{11})]\text{Ti}(\text{NMe}_2)_2$; instead, the deborated product $(\eta^5\text{-C}_2\text{B}_9\text{H}_{11})\text{Ti}(\text{NMe}_2)_2(\text{HNMe}_2)$ (**1**) was isolated in 29% yield. This compound was reported earlier from the reaction of $\text{C}_2\text{B}_9\text{H}_{13}$ with $\text{Ti}(\text{NMe}_2)_4$.¹¹ These reactions were closely monitored by the unique ^{11}B chemical shift (δ 36.1 ppm) of the bridging B atom in $\text{Pr}_2\text{NB}(\text{C}_9\text{H}_7)(\text{C}_2\text{B}_{10}\text{H}_{11})$.⁵ As indicated by ^{11}B NMR, such amine elimination reactions did not proceed at all at room temperature. Upon heating, **2** was formed cleanly, while the reaction of $\text{Ti}(\text{NMe}_2)_4$ with $\text{Pr}_2\text{NB}(\text{C}_9\text{H}_7)(\text{C}_2\text{B}_{10}\text{H}_{11})$ was very complicated. It was assumed that NMe_2^- in $\text{Ti}(\text{NMe}_2)_4$ might attack the bridging B atom and the cage B atom, leading to the formation of **1**. It was unlikely for the formed HNMe_2 to attack the B atoms; otherwise, **2** would not be isolated in high yield. These transformations are outlined in Scheme 1.

It had been known that treatment of $\text{Cp}_2\text{Zr}(\text{NMe}_2)_2$ with excess Me_3SiCl resulted in clean formation of Cp_2ZrCl_2 .¹² Reaction of **2** with excess Me_3SiCl led to the isolation of a zirconocene chloride compound $[\eta^5\text{-}\sigma\text{-Pr}_2\text{NB}(\text{C}_9\text{H}_7)(\text{C}_2\text{B}_{10}\text{H}_{11})]\text{ZrCl}_2$ (**4**) in 80% yield. Salt metathesis reaction between $\text{MCl}_4(\text{THF})_2$ and $[\text{Pr}_2\text{NB}(\text{C}_9\text{H}_7)(\text{C}_2\text{B}_{10}\text{H}_{11})]\text{Li}_2(\text{Et}_2\text{O})_2$ in a 1:1 molar ratio also afforded constrained-geometry compounds of the general formula $[\eta^5\text{-}\sigma\text{-Pr}_2\text{NB}(\text{C}_9\text{H}_7)(\text{C}_2\text{B}_{10}\text{H}_{11})]\text{MCl}_2$ ($\text{M} = \text{Ti}$ (**3**),

Scheme 2



Zr (**4**), **Hf** (**5**) in good yields. **3** was also prepared in 35% yield from the reaction of $[\text{Pr}_2\text{NB}(\text{C}_9\text{H}_7)(\text{C}_2\text{B}_{10}\text{H}_{11})]\text{Li}_2(\text{Et}_2\text{O})_2$ with 1 equiv of $\text{TiCl}_3(\text{THF})_3$ followed by addition of 0.5 equiv of PbCl_2 in THF. Interaction of **2** with 4 equiv of Me_3Al in toluene resulted in the isolation of the methyl derivative $[\eta^5\text{-}\sigma\text{-Pr}_2\text{NB}(\text{C}_9\text{H}_7)(\text{C}_2\text{B}_{10}\text{H}_{11})]\text{ZrMe}_2$ (**6**) in 78% yield. **6** was also prepared in 56% yield from the reaction of **4** with 2 equiv of MeLi in THF. These synthetic routes are summarized in Scheme 2.

These new constrained-geometry group 4 metal compounds were all very soluble in polar organic solvents such as THF, DME, and pyridine, sparingly soluble in toluene, and insoluble in *n*-hexane. They were fully characterized by various spectroscopic data and elemental analyses. The solid-state structures of compounds **1** and **2** were further confirmed by single-crystal X-ray analyses.

Spectroscopic Characterization. The ^1H NMR spectra show that compounds **1–6** are all unsolvated species. In addition to six multiplets observed in the aromatic region of the ^1H NMR spectra of **2–6**, there are two multiplets (~ 5.5 and ~ 3.3 ppm), four doublets in the region 0.5–1.3 ppm corresponding to two diastereotopic isopropanyl groups of the Pr_2N unit. This phenomenon is also observed in $[\eta^5\text{-}\sigma\text{-Pr}_2\text{NB}(\text{C}_9\text{H}_7)(\text{C}_2\text{B}_{10}\text{H}_{11})]\text{YN}(\text{SiHMe}_2)_2(\text{THF})_2$.⁵ The ^1H NMR spectrum of **2** also exhibits two singlets at 2.99 and 2.32 ppm attributable to two diastereotopic NMe_2 groups. These two singlets disappear upon treatment of **2** with excess Me_3SiCl , supporting the formation of **4**. A new singlet at -0.38 ppm (ZrMe_2 unit) is generated after reaction of **4** with 2 equiv of MeLi , confirming the formation of **6**. These results are in line with their ^{13}C NMR spectra. Their ^{11}B NMR spectra are similar, showing a 1:1:3:4:2 splitting pattern for **2–4** and a 1:1:3:6 splitting pattern for **5** and **6** (two resonances at higher field cannot be resolved), respectively. The IR spectra of **2–6** show a typical strong and broad characteristic B-H absorption

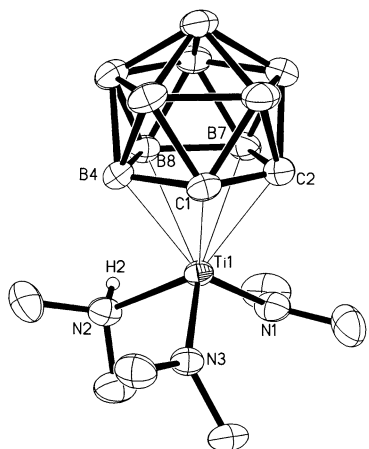
(11) Bowen, D. E.; Jordan, R. F.; Rogers, R. D. *Organometallics* **1995**, *14*, 3630.

(12) For examples, see: Diamond, G. M.; Jordan, R. F.; Petersen, J. L. *Organometallics* **1996**, *15*, 4045, and references therein.

Table 2. Key Structural Data for $[\eta^5\text{-}\sigma\text{-A}(\text{C}_9\text{H}_6)(\text{C}_2\text{B}_{10}\text{H}_{10})]\text{Zr}(\text{NMe}_2)_2$ and $[\eta^5\text{-}\sigma\text{-Me}_2\text{Si}(\text{C}_5\text{Me}_4)(\text{C}_2\text{B}_{10}\text{H}_{10})]\text{Zr}(\text{NMe}_2)_2$ (7)^a

A	Zr–C (C ₅ ring)	Zr–C (σ)	Zr–N	Cent–Zr–C(cage) ^b	C(C ₅ ring)–A–C(cage)	N–Zr–N	ref
^t Pr ₂ NB	2.522(2)	2.345(2)	2.026(2)	103.0	114.0(2)	106.4(1)	this work
Me ₂ C	2.521(8)	2.326(7)	2.016(8)	101.6	109.4(6)	108.0(3)	6
Me ₂ Si	2.541(5)	2.348(5)	2.019(4)	109.9	104.8(2)	107.3(2)	6
Me ₂ Si (7)	2.544(6)	2.355(5)	2.028(5)	110.3	105.8(2)	104.5(2)	18

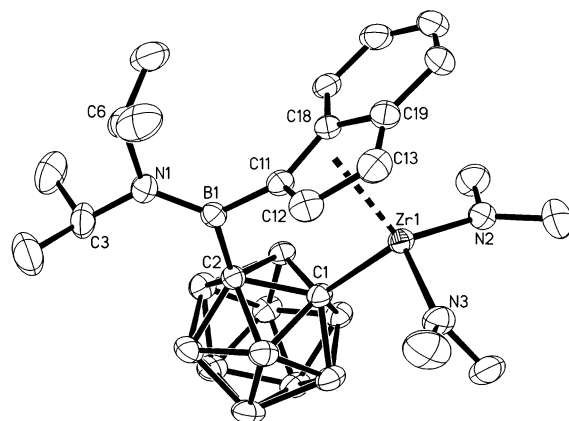
^a All distances are in Å and angles in deg. ^b Cent = centroid of the five-membered ring of the indenyl or tetramethylcyclopentadienyl group.

**Figure 1.** Molecular structure of $(\eta^5\text{-C}_2\text{B}_9\text{H}_{11})\text{Ti}(\text{NMe}_2)_2\text{-}(\text{HNMe}_2)$ (**1**) (thermal ellipsoids drawn at the 35% probability level).

at about 2560 cm^{-1} . The spectroscopic data of **1** are identical to those reported.¹¹

Molecular Structure. The solid-state structure of **1** derived from single-crystal X-ray analyses shows that it adopts a monomeric three-legged piano stool structure containing an η^5 -dicarbollide ligand with two amido and one amine ligand in the basal positions, a structure that is similar to $(\eta^5\text{-C}_2\text{B}_9\text{H}_{11})\text{Zr}(\text{NET}_2)_2(\text{HNMe}_2)$,¹¹ shown in Figure 1. The short Ti–N(1) and Ti–N(3) bond distances (1.886(2) and 1.913(2) Å) and the planar geometry around the N(1) and N(3) nitrogen atoms indicate that both nitrogen atoms with sp^2 hybridization are engaged in $\text{N}(\text{p}_\pi)\text{-Ti}(\text{d}_\pi)$ interactions. As expected, the Ti–N(2) distance of 2.215(2) Å is much longer than the Ti–N(amido) distance and the N(2) adopts a pyramidal geometry. The average Ti–cage atom distance is 2.423(2) Å. These structural data are very close to those found in $[(\eta^5\text{-C}_5\text{Me}_5)(\eta^5\text{-C}_2\text{B}_9\text{H}_{11})]\text{Ti}(\text{N}=\text{CMe}_2)$.¹³

The solid-state structure of **2** is shown in Figure 2. The Zr^{4+} ion is η^5 -bound to the five-membered ring of the indenyl group and σ -bound to two amido ligands and one cage carbon atom in a distorted-tetrahedral geometry. Both the bridging boron and nitrogen (N(1)) atoms are in a trigonal planar environment (sum of angles around N(1) and B(1) $\sim 360^\circ$). This geometry together with a short boron–nitrogen distance of 1.396(3) Å indicates the presence of a $\text{N}(\text{p}_\pi)\text{-B}(\text{p}_\pi)$ double-bond character. The B(bridging)–N (1.396(3) Å), B(bridging)–C(cage) (1.626(3) Å), and B(bridging)–C(ring) (1.587(3) Å) distances in **2** are very close to the corresponding values found in $[\eta^5\text{-}\sigma\text{-}^t\text{Pr}_2\text{NB}(\text{C}_9\text{H}_6)(\text{C}_2\text{B}_{10}\text{H}_{10})]_2\text{Ln}^{-5}$. The short Zr–N(2) and Zr–N(3) bond distances (2.041(2) and 2.011(2) Å) and the planar geometry around the N(2)

**Figure 2.** Molecular structure of $[\eta^5\text{-}\sigma\text{-}^t\text{Pr}_2\text{NB}(\text{C}_9\text{H}_6)\text{-}(\text{C}_2\text{B}_{10}\text{H}_{10})]\text{Zr}(\text{NMe}_2)_2$ (**2**) (thermal ellipsoids drawn at the 35% probability level).

and N(3) nitrogen atoms indicate that both nitrogen atoms with sp^2 hybridization are engaged in $\text{N}(\text{p}_\pi)\text{-Zr}(\text{d}_\pi)$ interactions. The lack of additional electron donation from the σ -carboranyl carbon atom to the Zr center also strengthens this $\text{N}(\text{p}_\pi)\text{-Zr}(\text{d}_\pi)$ interaction, resulting in substantial decrease in Zr–N bond distances compared with the corresponding Zr–N bond distances of 2.062(5) Å in $[\text{Me}_2\text{Si}(\text{C}_5\text{H}_4)(\text{NBu}^t)]\text{Zr}(\text{NMe}_2)_2$,¹⁴ 2.057(9) Å in $\text{rac-}[\text{C}_2\text{H}_4(\text{C}_9\text{H}_6)_2]\text{Zr}(\text{NMe}_2)_2$,¹⁵ 2.07 Å in $\text{Zr}(\text{NMe}_2)_4$,¹⁶ and 2.06 Å in $(\text{Me}_2\text{N})_2\text{Zr}(\mu\text{-NBu}^t)_2\text{-Zr}(\text{NMe}_2)_2$.¹⁷ For a comparison with similar constrained-geometry zirconium compounds, Table 2 summarizes the key structural data of $[\eta^5\text{-}\sigma\text{-Me}_2\text{A}(\text{C}_9\text{H}_6)(\text{C}_2\text{B}_{10}\text{H}_{10})]\text{-Zr}(\text{NMe}_2)_2$ with various linkage units A and $[\eta^5\text{-}\sigma\text{-Me}_2\text{Si}(\text{C}_5\text{Me}_4)(\text{C}_2\text{B}_{10}\text{H}_{10})]\text{Zr}(\text{NMe}_2)_2$.¹⁸ The cent–Zr–C(cage) angles increase in the order $\text{Me}_2\text{C} < {}^t\text{Pr}_2\text{NB} < \text{Me}_2\text{Si}$. The C(C₅ ring)–A–C(cage) angles decrease in the order ${}^t\text{Pr}_2\text{NB} > \text{Me}_2\text{C} > \text{Me}_2\text{Si}$. Other structural parameters are similar.

Ethylene Polymerization. Compounds **2–6** underwent preliminary testing for catalytic activity, using methylalumoxane (MAO) as cocatalyst (Al/cat. = 1500) in toluene at room temperature (1 atm of ethylene). The activity of $(\text{C}_5\text{H}_5)_2\text{ZrCl}_2$ was also tested under the same experimental conditions for comparison. The results are compiled in Table 3. All five compounds could catalyze the polymerization of ethylene with moderate to very high activities in the presence of MAO. Both the central metal ion and co-ligand affected the catalytic perfor-

(14) Carpenetti, D. W.; Kloppenburg, L.; Kupec, J. T.; Petersen, J. L. *Organometallics* **1996**, *15*, 1572.

(15) Christopher, J. N.; Diamond, G. M.; Jordan, R. F. *Organometallics* **1996**, *15*, 4038.

(16) Hagen, K.; Holwill, C. J.; Rice, D. A.; Runnacles, J. D. *Inorg. Chem.* **1988**, *27*, 2032.

(17) Nugent, W. A.; Harlow, R. L. *Inorg. Chem.* **1979**, *18*, 2030.

(18) Lee, M. H.; Hwang, J.-W.; Kim, Y.; Han, Y.; Do, Y. *Organometallics* **2000**, *19*, 5514.

(13) Kreuder, C.; Jordan, R. F.; Zhang, H. *Organometallics* **1995**, *14*, 2993.

Table 3. Ethylene Polymerization Results^a

catalyst	time (min)	yield (g)	activity (10 ⁶ g/(mol atm h))	$M_w/10^3$	M_w/M_n^c	T_m^d (°C)
(C ₅ H ₅) ₂ ZrCl ₂	60	3.75	1.25	103	2.28	130.0
2 (Zr)	60	0.60	0.20	465	14.0	135.5
3 (Ti)	60	0.22	0.07	372	21.5	131.3
4 (Zr)	10	1.97	3.94	346	2.88	137.0
4^b (Zr)	60	1.05	3.50	359	4.78	137.1
5 (Hf)	60	0.09	0.03	107	17.7	129.6
6 (Zr)	60	0.61	0.20	110	20.3	130.6

^a Conditions: toluene (50 mL), 1 atm of ethylene, $T = 25$ °C, catalyst (3.0 μ mol), MAO (4.5 mmol), Al/M = 1500. ^b Conditions: toluene (50 mL), 1 atm of ethylene, $T = 25$ °C, catalyst (0.3 μ mol), MAO (0.45 mmol), Al/Zr = 1500. ^c Measured by GPC (using polystyrene standards in 1,2,4-trichlorobenzene at 150 °C.) ^d Measured by DSC (heating rate: 10 °C/min).

mance of the catalysts, and the following trends were observed: (1) Zr \gg Ti > Hf and (2) Cl > Me \approx NMe₂. Note that two polymerization conditions were examined for **4** since a large amount of polyethylene precipitates caused difficulty in stirring. Among these catalysts, **4** exhibited the highest activity in ethylene polymerization. Its activity was slightly higher than the corresponding zirconium compounds derived from the Me₂C- and Me₂Si-bridged constrained-geometry ligands [Me₂A-(C₉H₅)(C₂B₁₀H₁₀)]²⁻ (Chart 1)⁶ and was at the high end for constrained-geometry metallocene catalysts reported in the literature.¹

The melting temperatures (T_m) of the polyethylenes prepared with the catalysts listed in Table 3 were between 129.6 and 137.1 °C, values typical for linear high-density polyethylenes. This result was supported by the IR spectra of the polymers showing no sign of branching.¹⁹ Molecular weights and polydispersities of the polymers produced ranged from 110 000 to 465 000 g mol⁻¹ and 2.88 to 20.3, respectively. These data indicated that **4** might be a single-site catalyst and the others might probably have more than one active site after activation with MAO.

(19) Koenig, J. L. *Chemical Microstructure of Polymer Chains*; Wiley: New York, 1982; p 63.

Conclusion

Several new group 4 metal compounds with a ⁱPr₂-NB-bridged constrained-geometry carboranyl ligand were prepared. They exhibited a moderate to very high ethylene polymerization activity when activated with MAO. The activities depended upon both the central metal ion and co-ligand. The following trends were observed: (1) Zr \gg Ti > Hf and (2) Cl > Me \approx NMe₂. Compound **4** showed the highest ethylene polymerization activity among the five compounds examined. This work also showed that the B-bridged system offered zirconium compounds with a slightly higher ethylene polymerization activity than the corresponding C- and Si-bridged systems, which might suggest that the ⁱPr₂-NB-linkage played a role in enhancing the catalytic activity of the resulting catalysts.

On changing from the Me₂A- (A = Si, C) to ⁱPr₂NB-linkage, Me₂A(C₉H₇)(C₂B₁₀H₁₁) (A = Si, C) and ⁱPr₂NB-(C₉H₇)(C₂B₁₀H₁₁) exhibited some different reactivity patterns. For example, the reaction of ⁱPr₂NB(C₉H₇)(C₂B₁₀H₁₁) with Ti(NMe₂)₄ did not give the expected compound [ⁱPr₂NB(C₉H₆)(C₂B₁₀H₁₀)]Ti(NMe₂)₂, while Ti(NMe₂)₄ reacted readily with Me₂A(C₉H₇)(C₂B₁₀H₁₁) (A = Si, C) to give the corresponding amide compounds in good yields.⁶ Unlike [Me₂A(C₉H₆)(C₂B₁₀H₁₀)]Zr(NMe₂)₂ (A = Si, C),⁶ treatment of [ⁱPr₂NB(C₉H₆)(C₂B₁₀H₁₀)]Zr(NMe₂)₂ with excess Me₃SiCl led to the complete conversion of the M(NMe₂)₂ moiety to the MCl₂ group.

Acknowledgment. We thank Prof. Diansheng Liu and Prof. Kevin Leung for the help in performing polymerization experiments. The work described in this paper was supported by grants from the Research Grants Council of the Hong Kong Special Administration Region (Project No. CUHK 4267/00P) and National Science Foundation of China through the Outstanding Young Investigator Award Fund (Project No. 20129002).

Supporting Information Available: Tables of crystallographic data and data collection details, atomic coordinates, bond distances and angles, anisotropic thermal parameters, and hydrogen atom coordinates and figures giving atom-numbering schemes for complexes **1** and **2**. This material is available free of charge via the Internet at <http://pubs.acs.org>.

OM020325J